Pergamon

Cement and Concrete Research 31 (2001) 933–939

CEMENT AND CONCRETE RESEARCH

Kinetics of dolomite–portlandite reaction Application to Portland cement concrete

S. Galí[a,*], C. Ayora[b], P. Alfonso[a], E. Tauler[a], M. Labrador[a]

[a]Departament de Cristal·lografia, Mineralogia i Dipòsits Minerals, Universitat de Barcelona, C/Martí i Franquès s/n, 08028 Barcelona, Catalunya, Spain
[b]Institut de Ciències de la Terra "Jaume Almera," CSIC, C/ Soler Sabarís s/n, 08028 Barcelona, Catalunya, Spain

Received 29 November 2000; accepted 6 March 2001

Abstract

The dedolomitization reaction kinetics are studied through several long-term experiments consisting of an aqueous dispersion of fine powders of dolomite and portlandite with different alkalinity, temperature and silica content. The experimental results are reproduced through computer simulation, which allows the estimation of the apparent dissolution constant rates for dolomite. These are discussed together with other parameters influencing the kinetics, in particular the modification of the specific surface of dolomite. The parameters obtained make it possible to predict the behavior of the system beyond experimental periods. Both experimental and simulated results are discussed in connection with the expansion and cracking occurrences observed in portland mortars and concretes made with dolomitic limestone.

Keywords: Kinetics; Alkali–aggregate reaction; Durability; Dolomite–portlandite; Simulation

1. Introduction

Expansion and cracking occurrences observed in concrete made of high-alkali portland cement and dolomitic limestone aggregate, have led to the supposition that an alkali–carbonate reaction (ACR) takes place [1,2], which accelerates the dedolomitization reaction. The reaction is supposed to proceed with an increase of volume of the resultant phases, or, alternatively, would produce the expansion of the bulk material through an indirect mechanism. The possible role of alkali in the dedolomitization reaction is still a controversial matter [3,4].

Many laboratory tests confirm that prisms of mortar made with dolomite aggregate expand after continuous attack by alkaline solutions [5], and this result has become the base for standard expansion tests in several countries. However, up to now, little evidence, if any, has been provided of an expansive reaction between alkali and dolomite.

In the dedolomitization reaction,

$$\mathrm{CaMg(CO_3)_2 + Ca(OH)_2 = 2CaCO_3 + Mg(OH)_2}$$

dolomite reacts with portlandite, producing calcite and brucite. Following the molar volumes of the solids involved [6], the reaction results in an increase of volume of 1.13%. According to the above authors, alkali would be needed only to form an intermediate alkali carbonate, but this point has not been proved yet. Other authors [7] and [8] claim that expansion observed would be produced through alkaline dissolution of silica or clay contained in the dolomitic aggregate (alkali–silica reaction, ASR). In this case, the ACR problem would lead us to the well-studied ASR problem.

Despite of the extensive research carried out in several laboratories, disagreement on the origin of the bulk expansion observed in concretes made of dolomitic aggregate still remains. In order to gain some insight on these problems at a more basic level, several long-term experiments on the evolution of media saturated with portlandite and dolomite were undertaken. These experiments include quantitative control of dissolution–precipitation of phases in different alkaline media, at 25°C and 75°C, and with silica content. All of these results are reproduced by computer simulation, and the

---

* Corresponding author. Tel.: +34-3-93-402-13-41; fax: +34-3-93-402-13-42.

E-mail address: gali@natura.geo.ub.es (S. Galí).

PII: S0008-8846(01)00499-9

kinetic parameter estimates allow the extension of the simulation to a wide variety of conditions.

2. Experimental

The basic batch experiments consisted of an aqueous dispersion of fine powders of the starting phases, dolomite and portlandite. Five different initial water solutions were used: (1) pure water at room temperature; (2) pure water at 75°C; (3) 0.1 molar NaOH solution at room temperature; (4) 0.1 molar NaOH solution at 75°C; and (5) as Experiment (1) pure water with silica, with low exposed surface, was also introduced in the batch dispersion.

The starting water solutions and mineral powders were introduced in Teflon bottles provided with a cap to avoid atmospheric carbonation. The volume ratio of starting minerals to solution (1/1000) was carefully chosen to facilitate further chemical analyses and, in particular, the filtration of the complete suspension, so that all the solids were recovered in the form of a thin film suitable for powder diffraction. Filters had 0.22 μm pore diameter.

About 10 to 15 bottles were prepared with the same starting composition. The content was stirred every 30 min. Bottles were extracted from the bath and opened after different periods of time. The period between two extractions was increased as the rate of reactions slowed down. The average duration of the experiments at room temperature, until a steady state was practically reached, was about 200 days. At 75°C, the steady state was reached earlier. In the following we give a brief description of the starting minerals and the methods of analysis.

2.1. Dolomite

Gem quality crystals of dolomite were finely powdered. Only the fraction of powder with diameter below 25 μm was used. The measured BET [9] surface was 2.12 $m^2 g^{-1}$. Powder diffraction showed a single phase. Electron microprobe analyses of the bulk solid confirmed the purity of the material.

2.2. Portlandite

"Alfa" commercial $Ca(OH)_2$ from Johnson Matthey was used. The measured BET surface was 16.5 $m^2 g^{-1}$. Powder diffractogram showed traces of $CaCO_3$, estimated to be under 1%.

Characterization of the filtered solution included pH measurement with a standard high alkalinity electrode, and cation analyses of the metals by Inductively Coupled Plasma-Atomic Emission Spectrometry (ICP-AES). The spectrometer used was a Perkin Elmer Elan 6000.

Quantitative analysis of the crystalline solids retained in the filters was achieved by the full diffraction profile matching method (quantitative Rietveld analysis), using the FULLPROF program [10]. When an amorphous phase was present, the composition was deduced by mass balance. Whenever necessary, the solids were also dissolved and analyzed by ICP-AES.

3. Chemical model

The calculations of the mineral–water reactions are based on the mass conservation equation in a closed system:

$$\frac{dc_i}{dt} = \sum_{m=1}^{N_R} \nu_{mi}^{R} \sigma_m k_m (\Omega_m - 1) \qquad i = 1\ldots N_C \qquad (1)$$

where c_i is the total concentration of the ith component in solution (kmol m^{-3}), and the right hand term of Eq. (1) is the amount of component supplied/scavenged by the dissolution/precipitation of minerals [11]. Thus, N_R is the number of minerals, ν_{mi}^{R} is the stoichiometric coefficient of the ith component in the dissolution reaction of the mth mineral, σ_m is its the specific reactive surface of the mineral ($m^2\ m^{-3}$), k_m is the growth or dissolution rate constant (kmol $m^{-2}\ s^{-1}$), obtained from experiments, and Ω_m is the saturation of the solution with respect to the mineral ($\Omega_m < 1$ for subsaturation, $\Omega_m > 1$ for supersaturation, and $\Omega_m = 1$ for equilibrium). The term in parentheses is the saturation-dependent term. As the solution reaches equilibrium the term in parenthesis in Eq. (1) tends to 0 and the dissolution of the mineral vanishes.

The total amount of component in solution, c_i, is distributed over various aqueous species (Table 1). By assuming chemical equilibrium between these species their concentration can be computed. See details of the calculation in Ref. [12]. The value of the saturation Ω_m is then calculated from the concentration of the species involved in the dissolution reaction.

Table 1
Chemical reactions considered in the chemical model

	log *K*
Primary aqueous species	
Ca^{2+}, Mg^{2+}, OH^-, CO_3^{2-}, $HSiO_3^-$	
Aqueous complexes	
$OH^- + H^+ = H_2O$	14.00
$HCO_3^- + OH^- = CO_3^{2-} + H_2O$	3.666
$CO_3Ca(aq) = Ca^{2+} + CO_3^{2-}$	− 3.327
$CaOH^+ = Ca^{2+} + OH^-$	− 1.145
$H_2SiO_4^{2-} = HSiO_3^- + OH^-$	− 1.036
$SiO_2\ (aq) + OH^- = HSiO_3^-$	4.042
Minerals	
$CaMg(CO_3)_2 = 2CO_3^{2-} + Ca^{2+} + Mg^{2+}$	− 1.709
$CaCO_3 = CO_3^{2-} + Ca^{2+}$	− 8.480
$Ca(OH)_2 = Ca^{2+} + 2OH^-$	− 5.435
$Mg(OH)_2 = Mg^{2+} + 2OH^-$	− 1.169
"Silica gel" $= HSiO_3^- + Ca^{2+} + OH^-$	− 8.548

The values of the equilibrium constants are those of the EQ3NR database [18].

The reactive surface area of a dissolving mineral is updated according to the decrease of its volume fraction ϕ_m:

$$\sigma_m(t+\Delta t)=\sigma_m(t)\left[\frac{\phi_m(t+\Delta t)}{\phi_m(t)}\right]^{\frac{2}{3}} \qquad (2)$$

Following Eq. (2), as the volume fraction of the mth mineral approaches zero, the reactive surface also approaches zero. Therefore, the dissolution of a mineral may vanish either because the solution reaches equilibrium or due to the exhaustion of the mineral.

The kinetics of calcite precipitation is described by the right hand term in Eq. (1). This term is consistent with the experimental law obtained by Inskeep and Bloom [13] for calcite precipitation at pH > 8 and $p_{\mathrm{CO}_2} < 0.01$ bar. A value of 3.90×10^{-7} mol m^{-2} s^{-1} for the rate constant was obtained from their experimental results. The same equation has been used to calculate the dissolution of dolomite. A rate constant value of 2.2×10^{-8} mol m^{-2} s^{-1} has been obtained from the experimental data of Refs. [14,15]. In the following calculations portlandite is assumed to dissolve faster than dolomite, while calcite and brucite precipitate in equilibrium. Therefore, the dissolution of dolomite is the slower reaction and controls the rate of the overall dedolomitization process.

4. Results

The general trend of the experimental results and the corresponding numerical simulation results are plotted in Figs. 1 and 2. Typically, the amount of solid phases, the composition of the solution and the pH were simulated as a function of time. The input data of the calculations are dissolution rate constants, and the initial specific surfaces

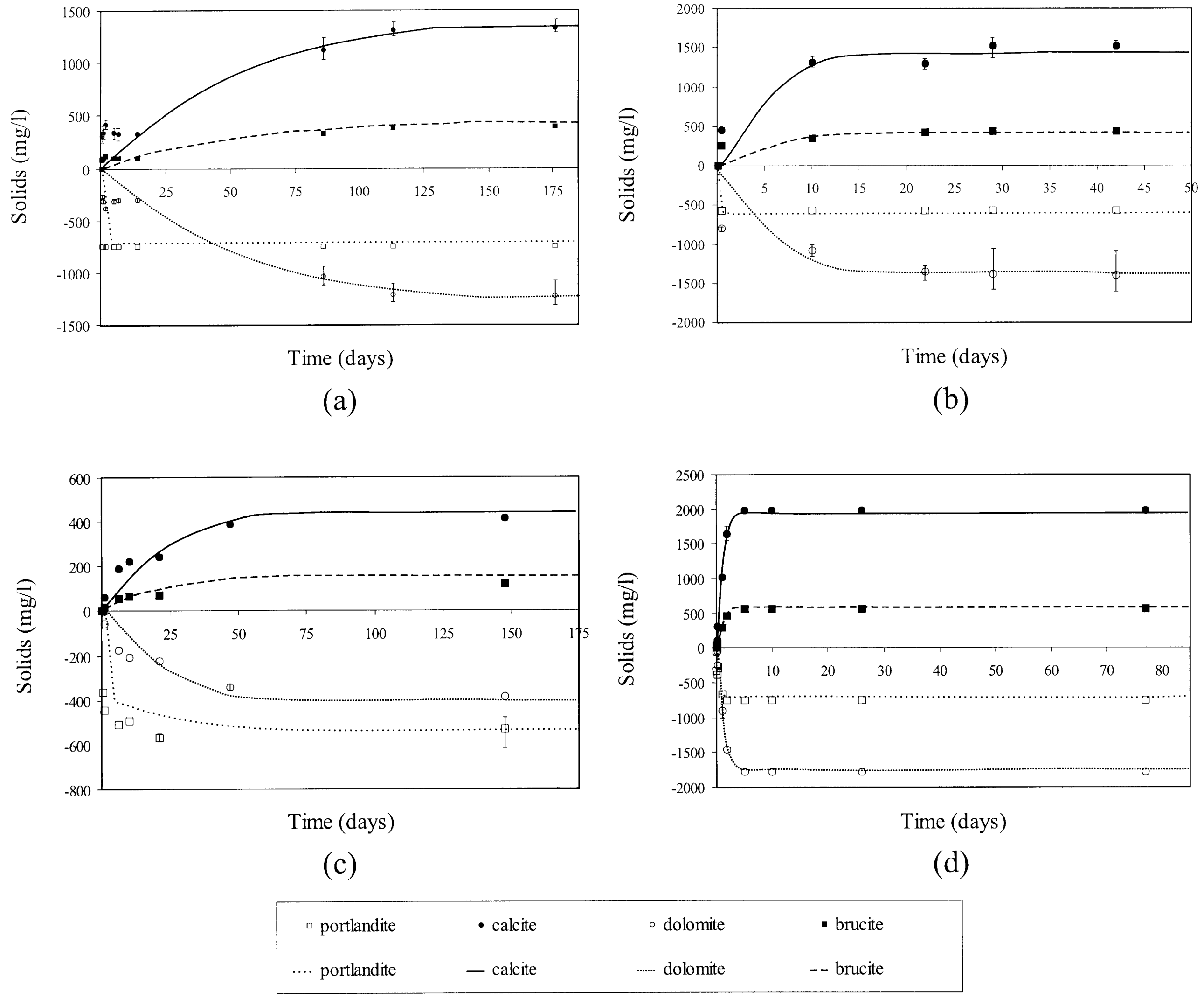

Fig. 1. Dissolved and precipitated solids. Different symbols indicate experimental values. Lines indicate simulated results. When error bars not drawn, the error is lower than the size of the symbols. (a) Experiment 1, final measured concentrations of Ca^{2+} and Mg^{2+} are 97.6 and 0.4 ppm, respectively. (b) Experiment 2, final measured concentrations of Ca^{2+} and Mg^{2+} are 2.8 and 5.4 ppm, respectively. (c) Experiment 3, final measured concentrations of Ca^{2+} and Mg^{2+} are 205.6 and 0.2 ppm, respectively. (d) Experiment 4, final measured concentrations of Ca^{2+} and Mg^{2+} are 1.5 and 0.1 ppm, respectively.

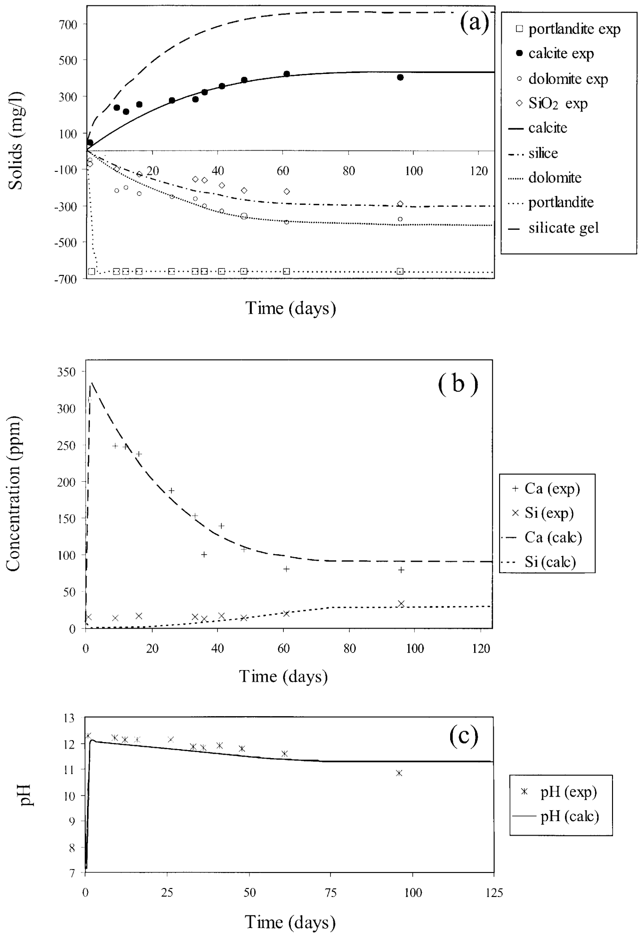

Fig. 2. Results obtained in Experiment 5. (a) Dissolved and precipitated solids. (b) Concentration of Ca^{2+} and Si^{4+}. (c) pH.

and volume fractions of the starting phases. In the following, we give a brief account of the main features of each group of experiments.

4.1. Pure water, 25°C (Fig. 1a)

At the beginning, the reaction takes place very quickly, probably consuming the finest fraction of dolomite powders. After 10 to 20 days, the reaction slows down, until a steady state is reached after 180 days. An apparent dissolution rate constant of 4.5×10^{-10} mol m^{-2} s^{-1} was obtained for dolomite by fitting the experimental results and the calculations. At the end of the experiment, dolomite was consumed almost completely (86%), and the solution remained subsaturated ($\Omega_{dol} = 5.0 \times 10^{-3}$). The steady state is reached because the reactive surface (σ_{dol}) has decreased to very small values.

4.2. Pure water, 75°C (Fig. 1b)

In this experiment, the equilibrium of the solution ($\Omega_{dol} = 1.0$) is reached after 15 days when 95% of dolomite is dissolved. The best-fit apparent dissolution rate constant for dolomite is 3.9×10^{-9} mol m^{-2} s^{-1}. By comparing the rate constants obtained in Experiments 1 and 2, activation energy of 37.2 kJ/mol is obtained for the dissolution reaction of dolomite. This value compares well with the range from 27.2 to 32.2 kJ/mol given in Ref. [16].

4.3. Solution 0.1 molar NaOH, 25°C (Fig. 1c)

The steady state is reached after 80 days when the reaction has only consumed 22.5% of the starting dolomite. The solution is subsaturated ($\Omega_{dol} = 0.26 \times 10^{-5}$), and the vanishing of the dissolution is due to the decrease of the reactive surface. From this point, the dissolution of dolomite will continue at a very slow rate, until the reaction is complete, after 400 days. An apparent dissolution rate constant of 2.3×10^{-10} mol m^{-2} s^{-1} is obtained from the comparison of analytical and calculated values. The high pH clearly slows down the dissolution of portlandite, which does not dissolve completely.

4.4. Solution 0.1 molar NaOH, 75°C (Fig. 1d)

The reaction ends after 5 days when portlandite and dolomite are completely exhausted and the only solids present are calcite and brucite. The dissolution rate constant for dolomite deduced from the experiment is 1.9×10^{-8} mol m^{-2} s^{-1}, almost an order of magnitude higher than the value obtained from Experiment 2. The activation energy deduced from Experiments 3 and 4 is 76.5 kJ/mol.

4.5. Pure water plus solid amorphous silica, 25°C (Fig. 2)

The most relevant reaction here is the formation of a calcium–magnesium silica gel, whose composition evolves with time. At high pH values amorphous silica dissolves fast and reacts with calcium and magnesium in solution, inhibiting the formation of calcite and preventing the formation of brucite, which is never observed. If reactive silica is in excess, portlandite is completely exhausted when only 23% of the starting dolomite is used up. The dissolution rate constants obtained for silica and dolomite are 1.5×10^{-8} mol m^{-2} s^{-1} and 2.1×10^{-10} mol m^{-2} s^{-1}, respectively.

5. Discussion

In all the experiments, the dedolomitization reaction progresses, in agreement with the well-known fact that the calcite–brucite pair is more stable than the dolomite–portlandite assemblage. In principle, the reaction should be complete with the consumption of one or both reactants, but this result was only achieved in experiments at 75°C.

At room temperature, the reaction proceeds very slowly after partial dissolution of dolomite. This was attributed to the decrease of the reactive surface between dolomite and water as dolomite is consumed. To confirm this point, single crystals of dolomite with dimensions 4 × 4 × 3 mm were immersed in portlandite-saturated solutions, with the same compositions as those in Experiments 1, 2 and 5. After several months, the surfaces of these crystals were observed and analyzed by SEM and XRD. In all cases calcite crystals were observed covering the surface of the dolomite crystals. Crystals of brucite were also present on the dolomite surface when silica was not present. In addition, diffraction showed that most calcite presented the same crystal orientation as dolomite, as expected, given the similarities between the structure of both minerals. It can be concluded, therefore, that the heterogeneous (mainly epitaxial) nucleation of calcite on the dolomite surface creates a protective layer inhibiting the dissolution of dolomite. The efficiency of this barrier may depend critically on temperature and alkali concentration: for 0.1 molar solution of NaOH, only 22.5% of dolomite was consumed after 80 days, at room temperature. On the contrary, at 75°C the reaction is completed after a few days.

In mortars the place where the new phases, calcite and brucite, are formed may be relevant with respect to the reported problems of expansion and cracking. The molar volumes of reactants and products indicate that the expansion of mortar with a volume content of 10% of portlandite could reach 0.33%, provided that all portlandite reacted with dolomite. Moreover, our observations indicate that part of the new phases would crystallize in the place occupied by dolomite. This observation suggests that one parameter determining the advance of the reaction is the total surface of contact between aggregate and paste. For millimeter-sized aggregates, or with bigger diameters (i.e., in mortars and concretes), the amount of exposed surface would depend mainly on the development of the layer of calcite surrounding the grains of dolomite. In addition, these new layer phases create an interface between the paste and the aggregate that may reduce the adherence, altering the mechanical properties of the concrete. This problem will be treated in a future paper.

Numerical simulation of the results is very useful since it allows the estimation of apparent dissolution rate constants of the phases involved. In the studied reactions, the best agreement between simulation and experiment is obtained by considering that the dissolution rate of portlandite is several orders of magnitude greater than that of dolomite, and that calcite and brucite precipitate in equilibrium with the solution. Therefore, the dissolution of dolomite is the slower process, and controls the overall reaction. The dissolution rate constant, k_{dol}, is obtained by fitting the calculated and observed results. The figures given above range from 2.1×10^{-10} to 4.5×10^{-10} mol m^{-2} s^{-1} for room temperature, two orders of magnitude lower than the value reported in the literature, 2.2×10^{-8} mol m^{-2} s^{-1} [14,15]. This discrepancy is interpreted as due to the precipitation of new phases, calcite and brucite, on the dolomite surface. This fact results in a decrease in the reactive surface with respect to that measured by BET. When k_{dol} is fitted only to the initial results (first 10 days) of Experiments 1 and 3, the obtained values are very similar to those given in the literature [14,15].

At room temperature, the addition of NaOH to the solution makes the reaction slower, while at high temperature alkali accelerates the reaction. The different activation energies obtained through Experiments 1–2 and 3–4 suggest that the mechanism of dissolution of dolomite, at a molecular level, would be different when alkali is present in the solution.

Numerical simulation also enables us to predict the behavior of the system beyond experimental time periods. Using the dissolution rates obtained for dolomite, we carried out the simulations for initial conditions similar to the actual interaction between aggregates and portlandite in mortars. For a cube of mortar with edge 1 dm, volume fractions and specific surfaces of aggregate and portlandite, and eventually reactive silica, were introduced in the code (Fig. 3a–e). The volume fraction of the interstitial pore solutions plus nonreactive phases was 0.3 and the initial compositions were the same as in Experiments 1 to 5. Neither carbonation from the atmosphere nor diffusion and transport limitations were considered. For reactions involving gel phases (Experiment 5), the volume is uncertain, and the simulated reaction will be more or less expansive depending on the molar volume attributed to these phases. For instance, the density of the C-S-H portland gel, depending on the different authors, may vary from 2.0 to 2.8 g cm^{-3} (see Ref. [17] for discussion). Using molar volume additive rules, the densities obtained for portlandite and calcium–magnesium silicate hydrate gel were 2.24 and 2.2 to 2.4 g cm^{-3}, respectively. Our results indicate that reactions involving the formation of gel increase slightly the total volume of solid, and are potentially expansive.

In the simulations depicted in Fig. 3a–d, corresponding to Experiments 1 to 4, the reaction ends when all portlandite is used up. This occurs after 200, 23, 390 and 4.7 years for initial compositions and temperatures similar to Cases 1 to 4. However, the diffusion barriers created during the process, not included in the simulation, may block the reaction early before equilibrium. On the other hand, it is noteworthy that the diffusion of atmospheric carbon dioxide can produce complete carbonation of the Portland paste in less than 100 years.

When silica is present (Fig. 3e), the evolution is less linear. As portlandite dissolves, pH is high and amorphous silica dissolves fast, forming a gel. After 130 years, portlandite is exhausted, but dissolution of dolomite and precipitation of calcite continues at a lower rate, at the expense of the calcium content of the gel. This becomes richer towards the brucite component, and, in equilibrium, antigorite-like minerals ($Mg_3[Si_2O_5]OH_4$) would crystallize.

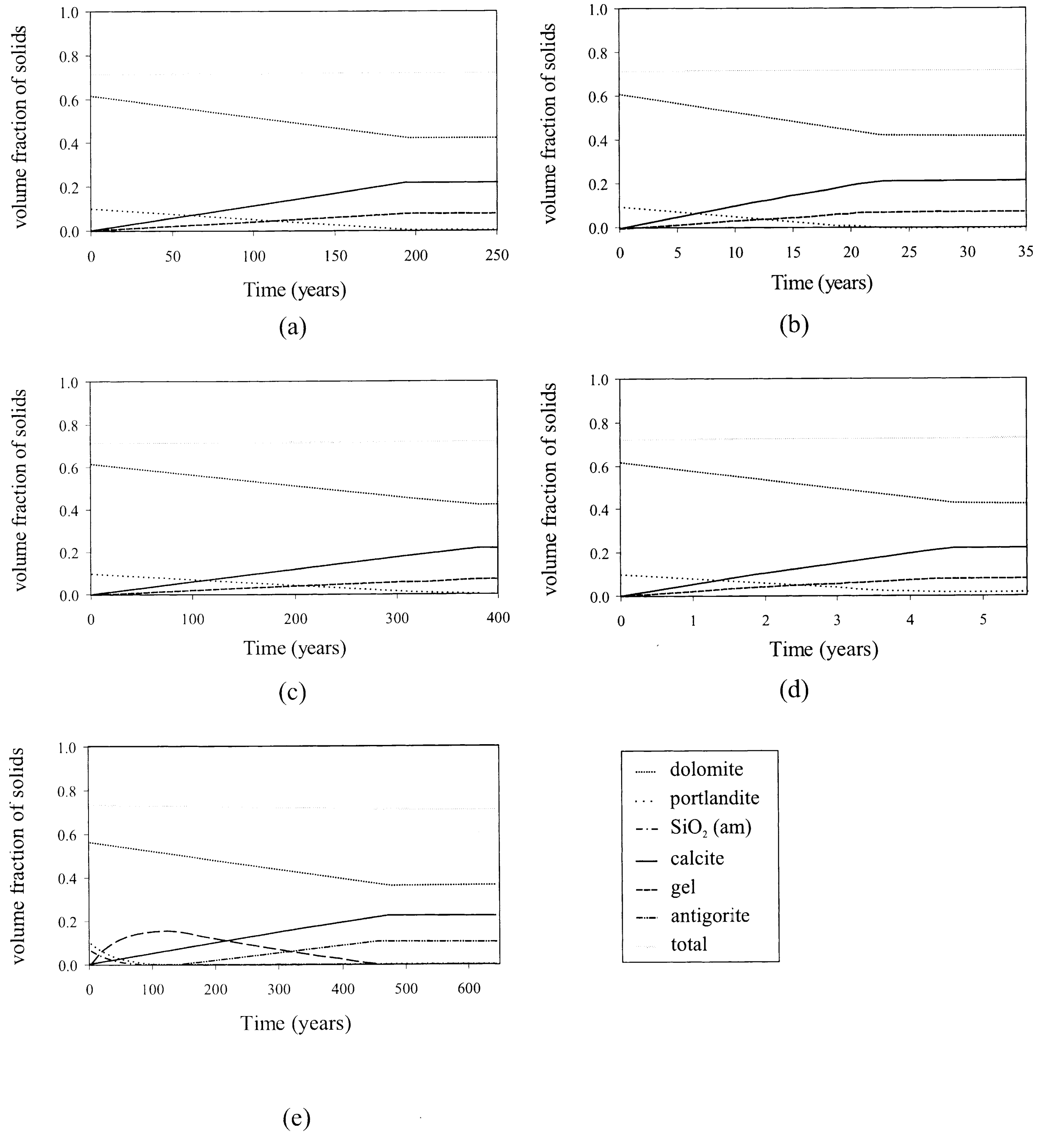

Fig. 3. Simulation of dissolved and precipitated solids for long periods of time, until the equilibrium between the different components is achieved. (a) Experiment 1, (b) Experiment 2, (c) Experiment 3, (d) Experiment 4, and (e) Experiment 5.

The evolution ends when all phases reach equilibrium with solution, after 460 years.

6. Conclusions

At room temperature, the apparent dissolution rates obtained for dolomite range from 2.1×10^{-10} to 4.5×10^{-10} mol m^{-2} s^{-1}. At 75°C, these values increase by more than one order of magnitude. The low values compared with those referred to in the literature are due to the decrease of the actual reactive surface caused by the precipitation of new solid phases.

The activation energies are similar to those of previous studies, suggesting that no significant differences in the dissolution mechanism took place. The activation energies, however, are influenced differently by the alkali content of the solution, indicating that a different mechanism of dissolution occurs when alkali is present.

At room temperature, alkali in the solution reduces the dissolution rate of dolomite. At 75°C, NaOH solution slightly increases the rate of the dedolomitization reaction.

Calcite and, possibly brucite, crystallize on the dolomite surface, reducing the surface and slowing down the reaction. In mortar and concrete the interface between the Portland paste and aggregate could be modified, affecting the mechanical properties of the material.

The total volume expansion produced in mortars by the complete reaction of portlandite with dolomite is estimated to be 0.33% (0.11% of linear expansion). At room temperature this expansion will be produced during a period of 200–400 years.

When reactive silica is present, the reaction of dedolomitization will continue long after portlandite is used up. The gel formed is potentially expansive, and changes its composition, towards the brucite component.

Acknowledgments

The ICP-AES analyses were performed at the Serveis Científico-Tècnics (SCT) de la Universitat de Barcelona. X-ray diffraction analyses were performed at the X-ray unit at the SCT (X. Alcobé). This research was sponsored by the CICYT Spanish research project MAT97-0380 and by DGR of the Catalan Government, under the project 98 BEA 1400412 and contract RED99-57.

References

[1] W.C. Hansen, Basic chemistry of reactions of aggregates in portland-cement concrete, ASTM J. Mater. 3 (1967) 408–431.

[2] E.G. Swenson, J.E. Gillott, Characteristics of Kingston carbonate rock reaction, Highw. Res. Board, Bull. 275 (1960) 18–31.

[3] J.E. Gillott, E.G. Swenson, Mechanism of the alkali–carbonate rock reaction, J. Eng. Geol. 2 (1969) 7–23.

[4] M.S. Tang, M. Deng, X. Lan, S. Han, Studies on alkali–carbonate reaction, ACI Mater. J. 91 (1) (1994) 26–29.

[5] L. Tong, M. Tang, Expandability of solid-volume-reducing reactions of alkali–magnesite and alkali–dolomite, Cem., Concr., Aggregates, CCAGDP 19 (1) (1997) 31–37.

[6] R.A. Robie, B.S. Hemingway, J.R. Fisher, Thermodynamic properties of minerals and related substances at 298.15 K and 1 bar (10^5 pascals) pressure and higher temperatures, U.S. Geol. Surv. 1452 (1978) 456 pp.

[7] J.E. Gillott, Alkali reactivity problems with emphasis on Canadian aggregates, Eng. Geol. 23 (1986) 29–43.

[8] T. Katayama, A critical review of carbonate rock reaction — is their reactivity useful or harmful?, Int. Conf. Alkali–Aggregate React. Concr., 9th, London, 2 (1992) 508–518.

[9] S. Brunnauer, P. Emmet, E. Teller, Adsorption of gases in multimolecular layers, J. Am. Chem. Soc. 60 (1938) 309–319.

[10] J. Rodriguez-Carvajal, FULLPROF, v. 3.2, Laboratoire Leon Brillouin (CEA-CNRS), 1998.

[11] A.C. Lasaga, Chemical kinetics of water–rock interactions, J. Geophys. Res., B 6 (1984) 4009–4025.

[12] C. Ayora, C. Taberner, M.W. Saaltink, J. Carrera, The genesis of dedolomites: A discussion based on textures and reactive transport modeling, J. Hydrol. 209 (1998) 346–365.

[13] W.P. Inskeep, P.R. Bloom, An evaluation of rate equations for calcite precipitation kinetics at $p\mathrm{CO}_2$ less than 0.01 atm and pH greater than 8, Geochim. Cosmochim. Acta 49 (1985) 2165–2180.

[14] E. Busenberg, L.N. Plummer, The kinetics of dissolution of dolomite in CO_2–H_2O systems at 1.5 to 65°C and 0 to 1 atm P_{CO_2}, Am. J. Sci. 282 (1982) 45–78.

[15] L. Chou, R.M. Garrels, R. Wollast, Comparative study of the kinetics and mechanisms of dissolution of carbonate minerals, Chem. Geol. 78 (1989) 269–282.

[16] J.S. Herman, W.B. White, Dissolution kinetics of dolomite; effects of lithology and fluid flow velocity, Geochim. Cosmochim. Acta 49 (10) (1985) 2017–2026.

[17] H.F.W. Taylor, Cement Chemistry, Academic Press, New York, 1990.

[18] T.J. Wolery, EQ3NR, a computer program for geochemical aqueous speciation–solubility calculations: Theoretical manual, user's guide and related documentation (Version 7.0), Publ. UCRL-MA-110662 Pt III, Lawrence Livermore Lab, Livermore, CA, USA, 1992.